land

MDPI

Article

Spatiotemporal Patterns and Driving Factors of Carbon Footprint in Coastal Saline Cropland Ecosystems: A Case Study of the Yellow River Delta, China

Yang Li [1,2,3], Dingwen Zhang [1,2], Ying Wen [4], Xiaoling Liu [1], Yi Zhang [1] and Guangmei Wang [1,*]

[1] Yantai Institute of Coastal Zone Research, Chinese Academy of Sciences, Yantai 264003, China; yangli@yic.ac.cn (Y.L.); dingwenzhang@yic.ac.cn (D.Z.); xiaolingliu@yic.ac.cn (X.L.); yizhang@yic.ac.cn (Y.Z.)
[2] University of Chinese Academy of Sciences, Beijing 101408, China
[3] Shandong Dongying Institute of Geographic Sciences, Dongying 257509, China
[4] Bureau of Agriculture and Rural Affairs of Fushan District, Yantai 265599, China; wenyingyx1991@163.com
* Correspondence: gmwang@yic.ac.cn

Abstract: Coastal saline cropland ecosystems are becoming increasingly vital for food security in China, driven by the decline in arable land and the growing demand for resource-intensive diets. Although developing and utilizing saline land can boost productivity, it also impacts greenhouse gas (GHG) emissions. This study uses the Yellow River Delta as a case study to analyze the spatial-temporal patterns of carbon footprints in saline croplands from 2001 to 2020 and their correlations with climate factors, cropland management scale, and agricultural mechanization. The results reveal that agricultural production in this region is characterized by high inputs, emissions, and outputs, with carbon emission efficiency improving significantly due to a reduction in net carbon emissions. Major sources of carbon emissions include electricity, chemical nitrogen fertilizers, nitrogen input, and straw return, which together account for 65.06% of total emissions. Based on these findings, three key principles have been proposed for policy recommendations to enhance carbon emission efficiency. First, adopt tailored strategies for regions with different salinization levels. Second, strengthen cropland drainage infrastructure to mitigate the adverse effects of heavy rainfall. Third, expand the scale of cropland management through land transfers and promote agricultural mechanization. These insights offer valuable guidance for mitigating GHG emissions in coastal saline cropland ecosystems.

Keywords: saline cropland ecosystem; carbon footprint; spatial-temporal pattern; driving factors; China

check for updates

Citation: Li, Y.; Zhang, D.; Wen, Y.; Liu, X.; Zhang, Y.; Wang, G. Spatiotemporal Patterns and Driving Factors of Carbon Footprint in Coastal Saline Cropland Ecosystems: A Case Study of the Yellow River Delta, China. *Land* **2024**, *13*, 2145. https://doi.org/10.3390/land13122145

Academic Editor: Claude Hammecker

Received: 4 November 2024
Revised: 4 December 2024
Accepted: 6 December 2024
Published: 10 December 2024

Copyright: © 2024 by the authors. Licensee MDPI, Basel, Switzerland. This article is an open access article distributed under the terms and conditions of the Creative Commons Attribution (CC BY) license (https://creativecommons.org/licenses/by/4.0/).

1. Introduction

In China, large tracts of saline land resources, including coastal tidal flats (>20,000 km^2), are dispersed throughout China's coastal zone [1]. However, one of the main threats to soil health that reduces land production is soil salinization [2]. In light of consumer preferences for diets that require more resources [3,4], China must effectively utilize its food-producing land, particularly the coastal saline cropland ecosystems that are progressively becoming more significant in maintaining food security. The degree of soil salinization may have an impact on greenhouse gas (GHG) emissions from cropland ecosystems [5]. The development and use of saline cropland ecosystems must take into account the GHG emissions of agricultural production in light of Sustainable Development Goal 13 ("Climate Action") and China's national strategies for carbon peaking and carbon neutrality targets. Particularly, increasing land productivity while not increasing GHG emissions should be the aim of the comprehensive development and utilization of saline–alkali land. Research on the spatial and temporal patterns of the coastal saline cropland ecosystem's GHG emissions and its driving factors could supply deep insight into emissions reduction.

The carbon footprint (CF) has gained popularity in cropland ecosystem research at various scales [6,7] and is a useful measurement technique for calculating GHG emissions [8,9]. It offers a scientific method for determining carbon budgets and locating possibilities for emission reduction by enabling the quantitative measurement of direct and indirect carbon emissions produced during a particular activity or throughout the course of a product's life cycle. Taking into account the cropland ecosystem as the border and the carbon footprint, carbon emissions in crop production primarily originate from the use of fertilizers, pesticides, plastic film, and other inputs, as well as from energy consumption such as fuel and electricity [9–11]. On the other hand, carbon absorption mainly occurs through practices such as applying organic fertilizers, returning straw to the field, and adopting no-tillage methods [9,10].

According to the CF calculation, agricultural inputs and practices directly impact the carbon emissions of cropland ecosystems. With the development of agricultural production, factors such as climate change, cropland management scale, and agricultural mechanization might have an increasingly significant effect on cropland ecosystems' carbon emissions. Concerning climate change, the extreme heat and drought during 1964–2007 caused a 9–10% reduction in global crop yield [12], giving rise to part of agricultural input (e.g., chemical nitrogen, pesticides) waste, which may lead to additional carbon emissions. Concerning the cropland management scale, different farm scale affects the agricultural inputs (e.g., labor, machinery input) [13], which also influences cropland ecosystems' carbon emissions. A previous study shows that large-scale cropland achieved lower carbon footprints compared to small households in non-saline cropland ecosystems [14]. Concerning agricultural mechanization, carbon emissions on the provincial scale of China would increase caused by agricultural mechanization [15]. However, the correlations between carbon emission and climate change, cropland management scale, and agricultural mechanization in the coastal saline cropland ecosystems have not been verified.

The Yellow River Delta has significant soil salinization and is typical of coastal saline land; meanwhile, it has a lot of potential to improve as a reserve of arable land. In recent years, the central government attaches great importance to not only saline–alkali soil improvement and productivity improvement but also the high-quality development of this region [16–19]. The GHG emissions from the Yellow River Delta's land use change points have been examined in earlier research. The primary source of carbon emissions from 2000 to 2019 was the cropland ecosystem; however, carbon emissions declined throughout that time [20]. Additionally, the Yellow River Delta wetland's soil CO_2 emission fluxes were examined [21]. However, the cropland ecosystem's GHG emissions and contributing variables have received less attention. What is the most effective strategy for reducing carbon emissions of the coastal saline cropland ecosystem, considering factors such as climate change, cropland management at different scales, and the level of agricultural mechanization?

This study uses the Yellow River Delta as a case study with the following specific objectives: (1) to analyze the temporal and spatial patterns of CF in the coastal saline cropland ecosystem and (2) to examine the relationships between CF and factors such as climate change (minimum temperature, maximum temperature, average temperature, annual precipitation, and annual evaporation), cropland management scale (arable land per capita of the rural population), and agricultural mechanization (machinery input per unit of arable land). In response to the above concerns, a CF quantitative model based on the life cycle assessment was built, and the data of the agricultural inputs and outputs in 2001–2020 of the Dongying City, Shandong Province, China, the main administrative region of Yellow River Delta, were used for calibration. First, a whole study-area analysis of the CF and its emission sources was conducted. Second, the comparisons of CF among the region types with different soil salinization were conducted. Third, the correlations between CF and different potential factors were identified. This study's key focuses are the ways in which cropland ecosystems have changed due to GHG emissions in recent decades and the factors that influence these changes in the Yellow River Delta region.

2. Materials and Methods

2.1. Study Area

Dongying City, the primary administrative center of the Yellow River Delta region in Shandong Province, China, as the research area (Figure 1), has relatively complete data to conduct our analysis. Based on the soil sampling in 2020 and combined with the second national soil survey, the spatial distribution of soil salinity was obtained by ArcGIS Desktop 10.6 (refer to Figure 1). Dongying City consists of 5 districts/counties, namely Dongying District, Hekou District, Kenli District, Lijin County, and Guangrao County. Dongying City has a moderate temperate continental monsoon climate, with an average annual temperature of 12.8 °C and 555.9 mm of precipitation. The arable land area is 22.92 × 10^4 hectares, and approximately 60% of the arable land is affected by soil salinization [22]. In 2020, the registered population was 197.96 × 10^4, the rural population accounted for 41.42%, and the total power of agricultural machinery reached to 2.72 × 10^6 kilowatt (KW) [22].

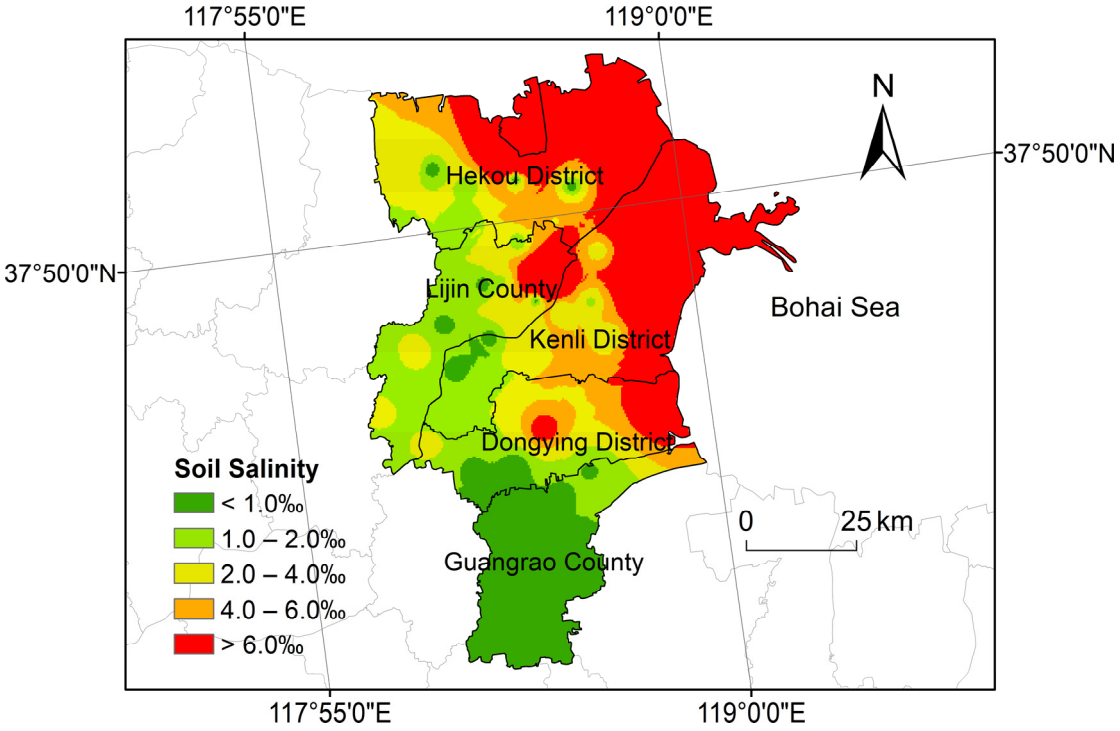


Figure 1. The location and the distribution of the 5 counties (Dongying District, Hekou District, Kenli District, Lijin County, and Guangrao County) for the study area. The soil salinity of Dongying City was based on the soil sampling in 2020.

2.2. System Boundary

The main crops cultivated in the area, including wheat, rice, maize, millet, sorghum, soybean, tuber, peanut, rape, sesame, cotton, vegetables, and melon, were analyzed using life cycle analysis (LCA) to build the CF estimation model [9]. The CF model took carbon sequestration and GHG emissions into account (Figure 2). The upstream and crop production sectors accounted for the majority of the GHG emissions. The agricultural inputs (chemical fertilizer (N, P, and K), pesticide, plastic film, electricity, and fuel) made up the majority of the upstream part, and the crop production section included direct and indirect emissions of CO_2, N_2O, and CH_4. According to a household questionnaire survey conducted in 2023, organic fertilizer is hardly used in crop production in the Yellow River Delta region; therefore, the increase in soil organic carbon from crop roots and straw returnis the primary carbon sequestration factor taken into account in this study.

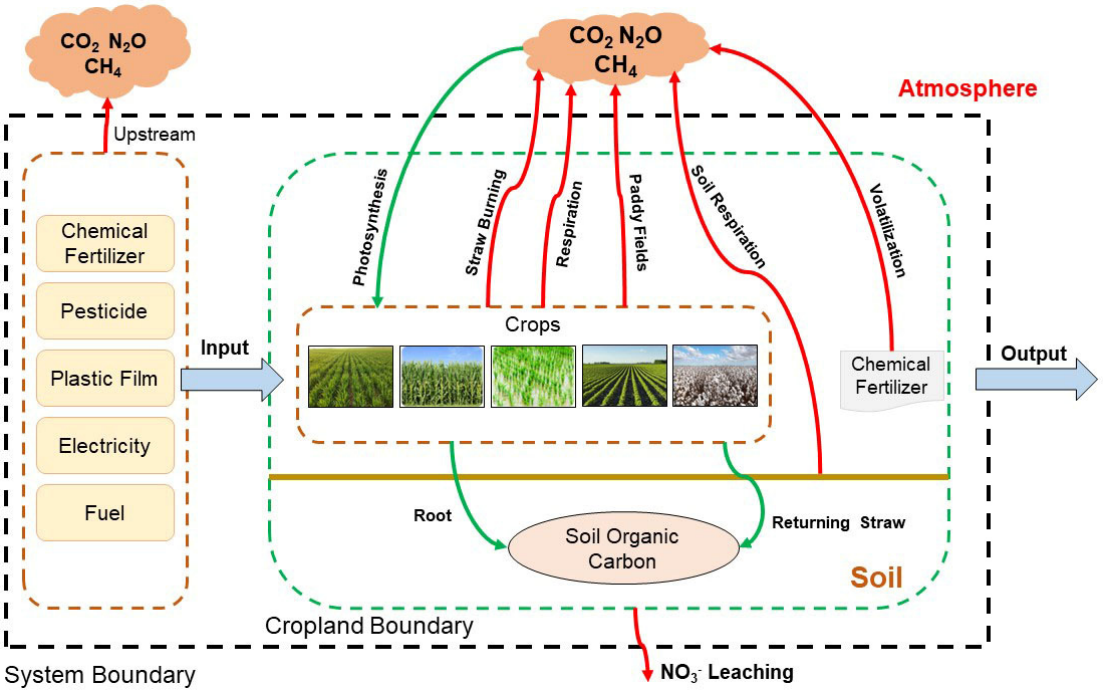


Figure 2. System boundary, GHG emissions, and carbon sequestration in a cropland ecosystem. Red arrows represent GHG emissions and green arrows represent carbon sequestration.

2.3. Carbon Footprint Quantification

2.3.1. GHG Emissions

The total GHG emissions of cropland ecosystems (TCE_j, ton CO_2-eq ha^{-1} yr^{-1}) mainly come from the upstream CO_2 equivalent of agricultural inputs (CE_{j,CO_2}, ton CO_2-eq ha^{-1} yr^{-1}), CO_2 emission equivalent from soil organic carbon loss by tillage ($CE_{j,tillage}$, ton CO_2-eq ha^{-1} yr^{-1}), CO_2 emission equivalent of N_2O emissions (CE_{j,N_2O}, ton CO_2-eq ha^{-1} yr^{-1}), and the CO_2 emission equivalent of CH_4 emissions (CE_{j,CH_4}, ton CO_2-eq ha^{-1} yr^{-1}). The TCE_j was calculated by the following equation:

$$TCE_j = CE_{j,CO_2} + CE_{j,tillage} + CE_{j,N_2O} + CE_{j,CH_4} \quad (1)$$

Concerning the upstream of agricultural inputs (i.e., chemical fertilizer (N, P, and K), pesticide, plastic film, electricity, and fuel), the total CO_2 equivalent in region j was calculated by the following equation:

$$CE_{j,CO_2} = \frac{\sum_{i=7}(AI_{i,j} \times EF_i)}{AA_j} \quad (2)$$

where $AI_{i,j}$ represents the quantity of agricultural inputs i in region j. There were 7 considered agricultural inputs. EF_i represents the CO_2 emission factor of the corresponding $AI_{i,j}$ (see Table 1). AA_j (ha) represents the arable area in region j.

Concerning the CO_2 emissions from soil organic carbon loss by tillage, we assumed that it is a constant value and that all arable land was tillage one time every year in the Yellow River Delta according to the traditional tillage. The $CE_{j,tillage}$ in region j was calculated by the following equation:

$$CE_{j,tillage} = LSOC_{tillage} \times \frac{44}{12} \quad (3)$$

where $LSOC_{tillage}$ represents the loss of soil organic carbon by tillage per unit of arable land per year by tillage. The molecular conversion factor of C to CO_2 is $\frac{44}{12}$. In this study, $LSOC_{tillage}$ was 0.04 ton ha^{-1} yr^{-1} [25].

Table 1. Emission factors of agricultural inputs.

Emission Source	Emission Factor (EF_i)	Reference
Chemical N fertilizer	7.76 ton CO_2 eq ton^{-1} N	[23]
Chemical P_2O_5 fertilizer	2.33 ton CO_2 eq ton^{-1} P_2O_5	[23]
Chemical K_2O fertilizer	0.66 ton CO_2 eq ton^{-1} K_2O	[23]
Pesticide	18 ton CO_2 eq ton^{-1} Pesticide	[7]
Fuel	3.75 ton CO_2 eq ton^{-1} Fuel	[24]
Plastic film	2.5 ton CO_2 eq ton^{-1} Plastic film	[6]
Electricity	1.14^{-3} ton CO_2 eq kwh^{-1}	[24]

Concerning the direct and indirect N_2O emissions, they mainly come from soil respiration, N input, atmospheric deposition of volatilized N, leaching and runoff of N, and returning crop straw. The total CO_2 equivalent of N_2O emissions in region j was calculated by the following equation:

$$CE_{j,N_2O} = \frac{(N_2O_{j,SR} + N_2O_{j,NI} + N_2O_{j,ADV} + N_2O_{j,RL} + N_2O_{j,CB})}{AA_j} \times \frac{44}{28} \times 273 \quad (4)$$

where $N_2O_{j,SR}$ represents the N_2O emissions from soil respiration without fertilization in region j; $N_2O_{j,NI}$ represents the N_2O emissions from N input (i.e., chemical N fertilizer and returning crop straw) in region j; $N_2O_{j,ADV}$ represents the N_2O emissions from the atmospheric deposition of volatilized N (i.e., chemical N fertilizer and returning crop straw) in region j; $N_2O_{j,RL}$ represents the N_2O emissions from leaching and runoff of N in region j; $N_2O_{j,CB}$ represents the N_2O emissions from crop straw burning in region j; the molecular conversion factor of N_2 to N_2O is $\frac{44}{28}$; the global warming potential of N_2O for the 100-year period is 273 [26]. For the detailed calculations of $N_2O_{j,SR}$, $N_2O_{j,NI}$, $N_2O_{j,ADV}$, $N_2O_{j,RL}$, and $N_2O_{j,CB}$, refer to Supplementary Materials.

Concerning the CH_4 emissions, they mainly come from paddy fields. The total CO_2 equivalent of CH_4 emissions was calculated by the following equation:

$$CE_{j,\ CH_4} = \frac{PCA_j \times EF_{CH_4} + CSB_j \times 0.25\%}{AA_j} \times \frac{16}{12} \times 29.8 \quad (5)$$

where PCA_j (ha) represents the area of the paddy field in region j. EF_{CH_4} (ton CH_4 ha^{-1} yr^{-1}) represents the CH_4 emission factor of the paddy field. In this study, the EF_{CH_4} is 0.234 ton CH_4 ha^{-1} yr^{-1} [27]. CSB_j represents the dry matter quantity of burned crop straw; the CH_4 emission factor of straw burning is 0.25% [9]; the molecular conversion factor of C to CH_4 is $\frac{16}{12}$; the global warming potential of CH_4 for the 100-year period is 29.8 [26].

2.3.2. Carbon Sequestration

Concerning the carbon sequestration by crop production systems in coastal saline cropland ecosystems, they mainly come from returning crop straw. The total carbon sequestration in region j (CS_j, ton CO_2-eq ha^{-1} yr^{-1}) was calculated by the following equation:

$$CS_j = \frac{CS_{j,RCS}}{AA_j} \times \frac{44}{12} \quad (6)$$

where $CS_{j,RCS}$ represents the carbon sequestration by returning crop staw; the molecular conversion factor of C to CO_2 is $\frac{44}{12}$. For the detailed calculation of $CS_{j,RCS}$, refer to Supplementary Materials.

2.3.3. Net Carbon Emissions, Energy Output, and Carbon Emission Efficiency

The net carbon emissions (NCE_j, ton CO_2-eq ha^{-1} yr^{-1}) in region j were the difference between TCE_j and the CS_j. The NCE_j was calculated by the following equation:

$$TCE_j = TCE_j - CS_j \tag{7}$$

The energy output in region j (EO_j, kJ ha^{-1} yr^{-1}) was defined as the sum of the energy produced by all crops. The energy productions considered in this study were the main crops in the Yellow River Delta region, including wheat, rice, maize, millet, sorghum, soybean, tuber, peanut, rape, sesame, cotton, vegetables, and melon. The EO_j was calculated by the following equation:

$$EO_j = \frac{\sum_k (Y_{k,j} \times EC_k)}{AA_j} \tag{8}$$

where $Y_{k,j}$ represents the production of crop k in region j and EC_k (kJ ton^{-1}) represents the energy conversion coefficient of crop k (see Table S4).

In this study, we defined the carbon emission efficiency (CEE) as the energy production of crops per unit carbon emissions. The carbon emission efficiency in region j (CEE_j, kJ $g^{-1}CO_2$-eq yr^{-1}) was calculated by the following equation:

$$CEE_j = \frac{EO_j}{TCE_j} \tag{9}$$

The larger CEE_j, the higher the carbon emission efficiency of region j.

2.4. Data

The basic data, including arable land area, agricultural inputs, cultivated area of crops, and crop yield during 2001–2020 were obtained from the Dongying City Statistical Yearbook. In several years, data have been unavailable (i.e., 2008–2010 and 2017); however, it would not make a big difference in the results considering the long timescale (2001–2020). The climate data of minimum temperature, maximum temperature, average temperature, annual precipitation, and annual evaporation came from ERA5-Land monthly averaged data [28] and were addressed by Google Earth Engine. Other coefficient data used in this study were specified in the corresponding content.

2.5. Spatial Analysis

The soil is more salinized near the sea and less so far from the coast [29] (Figure 1). The soil salinity of Kenli District (average value: 12.80‰) is the highest, followed by Hekou District (average value: 6.95‰), Lijin County (average value: 4.05‰), and Dongying District (average value: 3.77‰), and Guangrao County (average value: 0.97‰) is almost unaffected by soil salinization. The degree of soil salinization could affect the agricultural inputs and outputs. To analyze the performance of carbon emissions in different soil salinization regions, we first divided the regions according to the soil salinity level, i.e., high salinization regions (>6.00‰, Kenli District and Hekou District), moderate salinization regions (3.00–6.00‰, Lijin County and Dongying District), and low salinization regions (<3.00‰, Guangrao County), then we analyze the trend changes in carbon emissions in different region types according to soil salinization.

2.6. Factor Analysis

Pairwise correlation indices using Spearman correlation analysis were calculated among carbon emission indices and climate factors (minimum temperature, maximum

temperature, average temperature, and annual precipitation), cropland management scale (arable land per capita of rural population), and agricultural mechanization (machinery input per unit arable land). Strong positive correlations are indicated by correlation index values larger than 0.50, whereas strong negative correlations are indicated by values less than −0.50. Significant correlations were only taken into account if their *p*-value was less than 0.05.

3. Results

3.1. Carbon Emissions of the Whole Study Area

3.1.1. Carbon Emission Sources

During 2001–2020, the carbon emission sources of the coastal saline cropland ecosystem were mainly the agricultural input, tillage, N_2O emissions, and CH_4 emissions. Concerning the agricultural input, the change trend showed a significant downward trend (−0.0802 ton CO_2-eq ha^{-1} yr^{-1}, $R^2 = 0.2948$, $p < 0.05$) (Figure 3a and Table 2), which was caused by the downward trend of chemical N fertilizer (−0.0621 ton CO_2-eq ha^{-1} yr^{-1}, $R^2 = 0.6732$, $p < 0.01$), chemical P fertilizer (−0.0054 ton CO_2-eq ha^{-1} yr^{-1}, $R^2 = 0.3254$, $p < 0.05$), and plastic film (−0.0042 ton CO_2-eq ha^{-1} yr^{-1}, $R^2 = 0.5589$, $p < 0.01$). The average value of carbon emission was highest in chemical N fertilizer (2.16 ton CO_2-eq ha^{-1}), followed by electricity (2.15 ton CO_2-eq ha^{-1}), fuel (0.57 ton CO_2-eq ha^{-1}), pesticide (0.39 ton CO_2-eq ha^{-1}), and chemical P fertilizer (0.36 ton CO_2-eq ha^{-1}), and the average values were lowest in plastic film (0.10 ton CO_2-eq ha^{-1}) and chemical K fertilizer (0.10 ton CO_2-eq ha^{-1}).

Concerning the N_2O emissions, the change showed a significant downward trend (−0.1183 ton CO_2-eq ha^{-1} yr^{-1}, $R^2 = 0.8348$, $p < 0.01$), which was mainly caused by the downward trends of nitrogen input (−0.0399 ton CO_2-eq ha^{-1} yr^{-1}, $R^2 = 0.6909$, $p < 0.01$), atmospheric deposition (−0.0043 ton CO_2-eq ha^{-1} yr^{-1}, $R^2 = 0.6867$, $p < 0.01$), leaching and runoff (−0.0102 ton CO_2-eq ha^{-1} yr^{-1}, $R^2 = 0.6867$, $p < 0.01$), and burning (−0.0571 ton CO_2-eq ha^{-1} yr^{-1}, $R^2 = 0.8333$, $p < 0.01$) (Figure 3c). The average value of carbon emissions was highest in nitrogen input (1.52 ton CO_2-eq ha^{-1}), followed by returning straw (1.06 ton CO_2-eq ha^{-1}), burning (0.77 ton CO_2-eq ha^{-1}), and leaching and runoff (0.41 ton CO_2-eq ha^{-1}), and the average value was lowest in atmospheric deposition (0.17 ton CO_2-eq ha^{-1}).

Concerning the CH_4 emissions, the change was not significant. However, the CH_4 emissions of burning showed a significant downward trend (−0.0203 ton CO_2-eq ha^{-1} yr^{-1}, $R^2 = 0.7977$, $p < 0.01$). The average value of carbon emissions was highest in paddy fields (0.50 ton CO_2-eq ha^{-1}) and was lowest in burning (0.30 ton CO_2-eq ha^{-1}). For the CH_4 emissions of paddy fields, there was a sudden rise point in 2014, which may relate to the increase in the rice cultivated area. Concerning the tillage, the carbon emissions were less and the trend change was not significant.

Table 2. Interannual trends of various agricultural emission sources based on linear regression.

Emission Sources	Regression Equation	R^2	*p*-Value
Agricultural Input	y = −0.0802x + 167.001	0.2948	**0.03**
N	y = −0.0621x + 127.066	0.6732	**<0.01**
P	y = −0.0054x + 11.199	0.3254	**0.02**
K	y = 0.0002x − 0.382	0.0270	0.55
Plastic Film	y = −0.0042x + 8.476	0.5589	**<0.01**
Fuel	y = −0.0114x + 23.505	0.2345	0.06
Pesticide	y = −0.0046x + 9.591	0.0775	0.30
Electricity	y = 0.0073x − 12.455	0.0305	0.52
Tillage	/		

Table 2. *Cont.*

Emission Sources	Regression Equation	R^2	*p*-Value
N_2O	y = −0.1183x + 241.832	0.8348	**<0.01**
Returning Straw	y = −0.0068x + 14.759	0.1805	0.10
Nitrogen Input	y = −0.0399x + 81.702	0.6909	**<0.01**
Atmospheric Deposition	y = −0.0043x + 8.752	0.6867	**<0.01**
Leaching and Runoff	y = −0.0102x + 21.005	0.6867	**<0.01**
Burning_N_2O	y = −0.0571x + 115.614	0.8333	**<0.01**
CH_4	y = 0.0027x − 4.633	0.0043	0.81
Paddy	y = 0.0229x − 45.689	0.2452	0.05
Burning_CH_4	y = −0.0203x + 41.055	0.7977	**<0.01**

Note: Bolded values in the table indicate significant trend changes, where the *p*-value is less than 0.05.

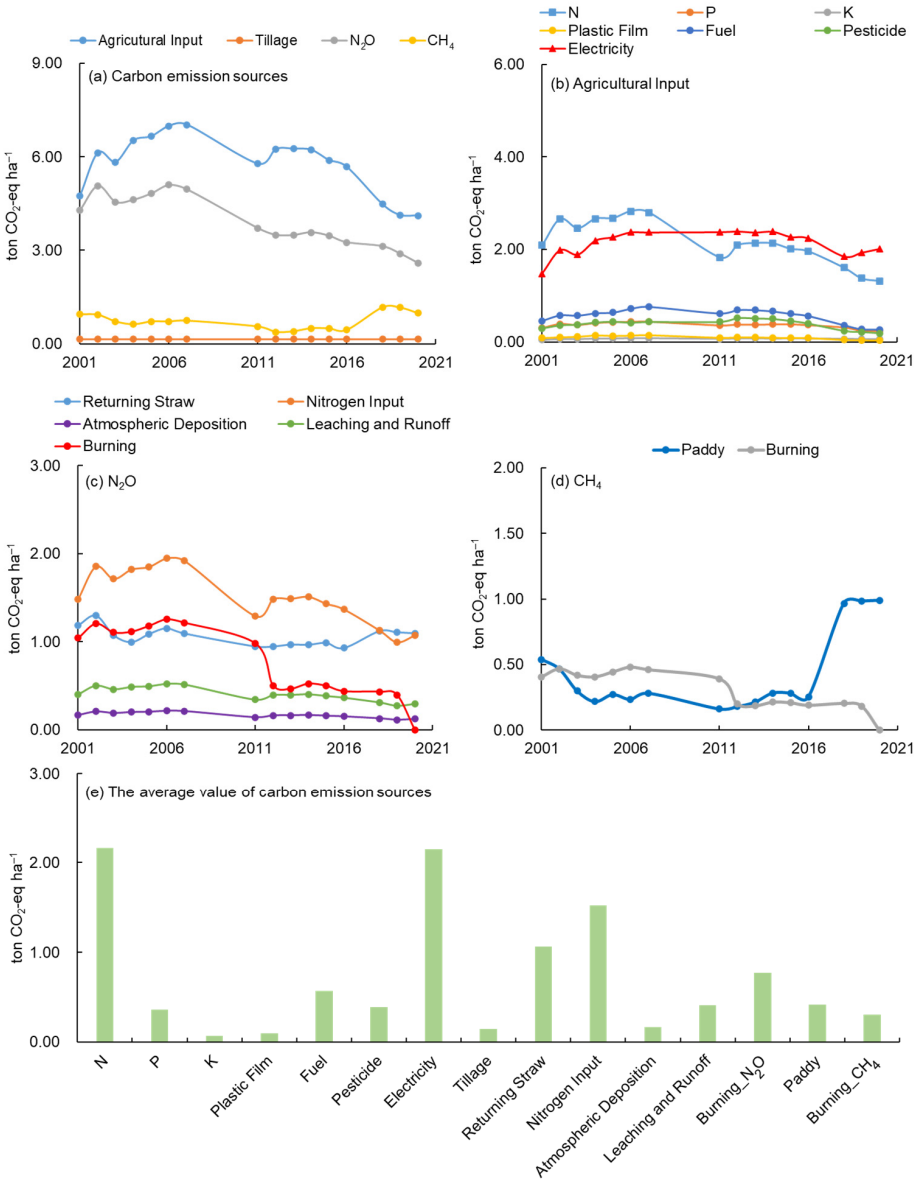


Figure 3. Variations of carbon emission sources (**a**), agricultural input (**b**), N_2O emissions (**c**), and CH_4 emissions (**d**) in the whole Yellow River Delta region during 2001–2020. (**e**) The average values of carbon emission sources during 2001–2020.

3.1.2. Carbon Emission Indices

During 2001–2020, carbon emissions (-0.1955 ton CO_2_eq ha^{-1}, $R^2 = 0.6438$, $p < 0.01$) and net carbon emissions (-0.1939 ton CO_2_eq ha^{-1}, $R^2 = 0.644$, $p < 0.01$) showed downward trends in the whole Yellow River Delta region (Figure 4). Table 2 shows that the decrease in carbon emissions is primarily attributed to the reduction in agricultural inputs and N_2O emissions, including declines in N, P, and plastic film, as well as a reduction in N_2O emissions from nitrogen input, atmospheric deposition, leaching and runoff, and burning. Considering the change trends of carbon sequestration and energy output were not significant, the carbon emissions efficiency (0.2467 KJ g^{-1} CO_2_eq, $R^2 = 0.5413$, $p < 0.01$) increased significantly. The average values were 10.60 ton CO_2_eq ha^{-1} for carbon emissions, 0.35 ton CO_2_eq ha^{-1} for carbon sequestration, 10.25 ton CO_2_eq ha^{-1} for net carbon emissions, 9.52×10^7 KJ ha^{-1} for energy output, and 9.55 KJ g^{-1} CO_2_eq for carbon emission efficiency.

3.2. Carbon Emission Indices in Different Region Types of Soil Salinization

Differences in carbon emission indices of different region types with soil salinization existed in 2001–2020 (Table 3). Concerning the carbon emissions, the average value in low-salinization regions (15.62 ton CO_2-eq ha^{-1}) was higher than in moderate—(9.75 ton CO_2_eq ha^{-1}) and high—(6.37 ton CO_2_eq ha^{-1}) salinization regions ($p < 0.01$). The carbon emissions of low-salinization regions (-0.349 ton CO_2_eq ha^{-1} yr^{-1}, $p < 0.01$) and moderate salinization regions (-0.195 ton CO_2_eq ha^{-1} yr^{-1}, $p < 0.01$) showed significant downward trends. Concerning the carbon sequestration, the average value in low-salinization regions (0.61 ton CO_2_eq ha^{-1}) was higher than in moderate—(0.36 ton CO_2_eq ha^{-1}) and high—(0.15 ton CO_2_eq ha^{-1}) salinization regions. The carbon sequestration of low-salinization regions showed a decreasing trend (-0.009 ton CO_2_eq ha^{-1} yr^{-1}, $p < 0.01$), while the high-salinization regions (0.003 ton CO_2_eq ha^{-1} yr^{-1}, $p < 0.05$) showed a significant increasing trend. Concerning the net carbon emissions, the average value in low-salinization regions (15.01 ton CO_2_eq ha^{-1}) was higher than in moderate—(9.40 ton CO_2_eq ha^{-1}) and high- (6.22 ton CO_2_eq ha^{-1}) salinization regions. The net carbon emissions of low-salinization regions (-0.339 ton CO_2_eq ha^{-1} yr^{-1}, $p < 0.01$) and moderate-salinization regions (-0.195 ton CO_2_eq ha^{-1} yr^{-1}, $p < 0.01$) showed significant downward trends. Concerning the energy output, the average value in low-salinization regions (16.65×10^7 kJ ha^{-1}) was higher than in moderate—(8.60×10^7 kJ ha^{-1}) and high—(4.91×10^7 kJ ha^{-1}) salinization regions. The change trends of energy output in different salinization regions were not significant. Regarding carbon emission efficiency, the average value in low-salinization regions (11.33 kJ $g^{-1}CO_2$_eq) was higher than in high-salinization regions (8.23 kJ $g^{-1}CO_2$_eq). However, no significant difference was observed between low- and moderate-salinization regions, as well as between high- and moderate-salinization regions. The change trends of carbon emission efficiency in high-salinization regions (0.184 kJ $g^{-1}CO_2$_eq yr^{-1}, $p < 0.05$), moderate-salinization regions (0.372 kJ $g^{-1}CO_2$_eq yr^{-1}, $p < 0.01$), and low-salinization regions (0.213 kJ $g^{-1}CO_2$-eq yr^{-1}, $p < 0.01$) all increased significantly.

Table 3. Spatial characteristics of carbon emission dynamics across regions with different salinization levels.

Indices		High-Salinization Regions	Moderate-Salinization Regions	Low-Salinization Regions
Carbon emissions	2001 (ton CO_2-eq ha^{-1})	6.27	9.26	14.36
	2020 (ton CO_2-eq ha^{-1})	6.02	6.87	11.01
	Average value (ton CO_2-eq ha^{-1})	6.37c	9.75b	15.62a
	Annual variation (ton CO_2-eq ha^{-1} yr^{-1})	−0.025	**−0.195**	**−0.349**
	R^2	0.08	0.63	0.64
	p-value	0.28	0.00	0.00

Table 3. *Cont.*

Indices		High-Salinization Regions	Moderate-Salinization Regions	Low-Salinization Regions
Carbon sequestration	2001 (ton CO_2-eq ha^{-1})	0.16	0.30	0.61
	2020 (ton CO_2-eq ha^{-1})	0.25	0.44	0.59
	Average value (ton CO_2-eq ha^{-1})	0.15c	0.36b	0.61a
	Annual variation (ton CO_2-eq ha^{-1} yr^{-1})	**0.003**	0.000	**−0.009**
	R^2	0.25	0.00	0.50
	p-value	0.05	0.90	0.00
Net carbon emissions	2001 (ton CO_2-eq ha^{-1})	6.11	8.96	13.75
	2020 (ton CO_2-eq ha^{-1})	5.77	6.42	10.42
	Average value (ton CO_2-eq ha^{-1})	6.22c	9.40b	15.01a
	Annual variation (ton CO_2-eq ha^{-1} yr^{-1})	−0.028	**−0.195**	**−0.339**
	R^2	0.10	0.64	0.63
	p-value	0.23	0.00	0.00
Energy output	2001 (10^7 kJ ha^{-1})	5.77	8.15	15.46
	2020 (10^7 kJ ha^{-1})	7.29	10.71	14.50
	Average value (10^7 kJ ha^{-1})	4.91c	8.60b	16.65a
	Annual variation (10^7 kJ ha^{-1} yr^{-1})	0.095	0.089	−0.081
	R^2	0.17	0.15	0.11
	p-value	0.12	0.13	0.22
Carbon emission efficiency	2001 (kJ $g^{-1}CO_2$-eq)	9.80	9.14	11.24
	2020 (kJ $g^{-1}CO_2$-eq)	12.38	16.89	13.92
	Average value (kJ $g^{-1}CO_2$-eq)	8.23b	9.86ab	11.33a
	Annual variation (kJ $g^{-1}CO_2$-eq yr^{-1})	**0.184**	**0.372**	**0.213**
	R^2	0.26	0.62	0.76
	p-value	0.05	0.00	0.00

Note: Bolded values in the table indicate significant trend changes, where the *p*-value is less than 0.05.

3.3. Correlations Among Carbon Eission Indices and Other Factors

The correlations between carbon emission indices and other factors are presented in Figure 5. Strong and positive connections were indicated by the correlation index r values between the carbon emissions, carbon sequestration, and net carbon emissions, all of which were higher than 0.51 with regard to the carbon emissions indices. As a result, there is a synergic relationship between carbon emissions, net carbon emissions, and carbon sequestration in the Yellow River Delta region. The carbon emission efficiency was strongly and negatively correlated with carbon emissions (r = −0.85) and net carbon emissions (r = −0.85), while it was strongly and positively correlated with energy output (r = 0.61), which was determined by the formula.

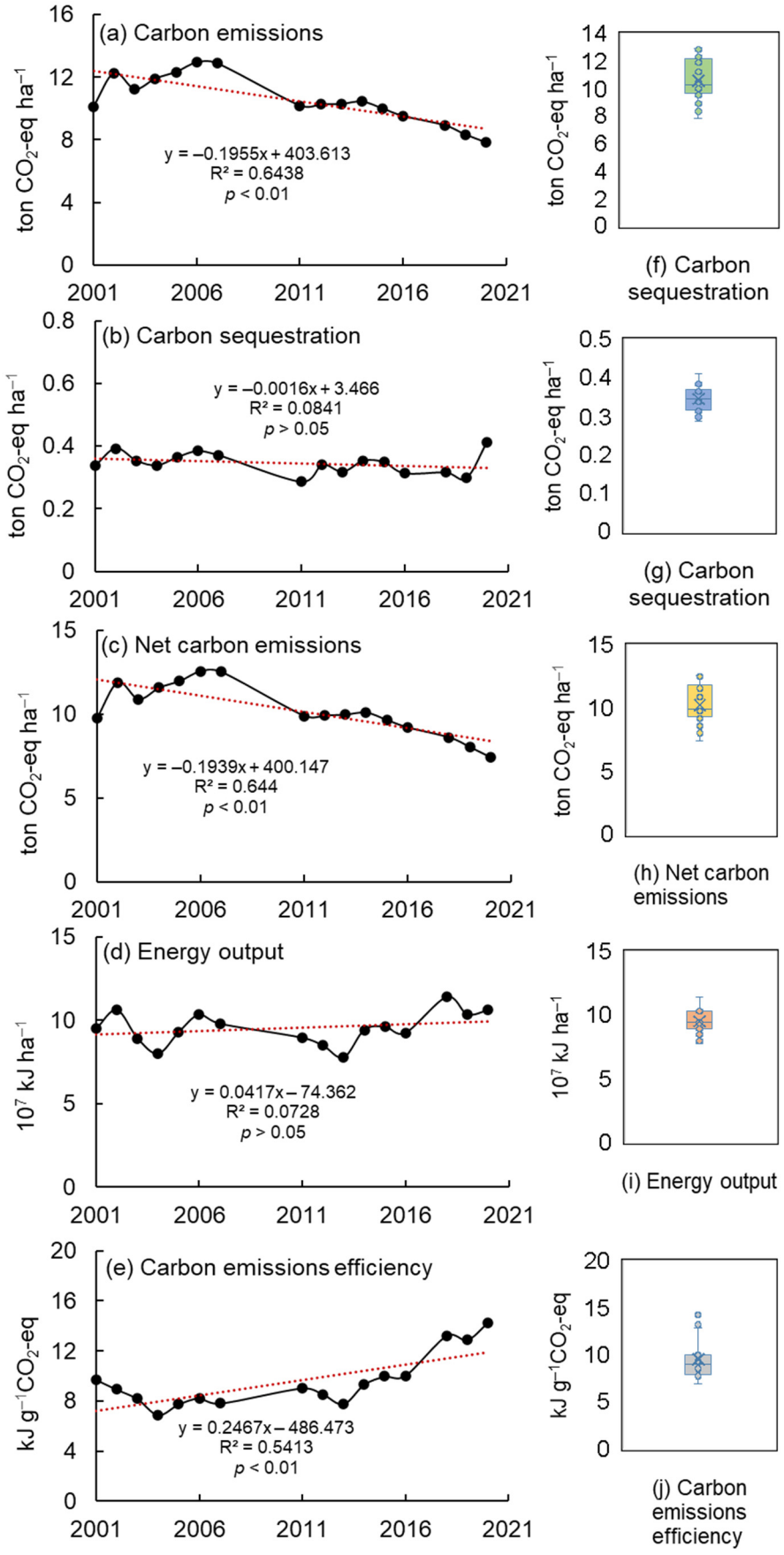


Figure 4. Variations and boxplots of carbon emissions (**a**,**f**), carbon sequestration (**b**,**g**), net carbon emissions (**c**,**h**), energy output (**d**,**i**), and carbon emission efficiency (**e**,**j**) for the whole Yellow River Delta region.

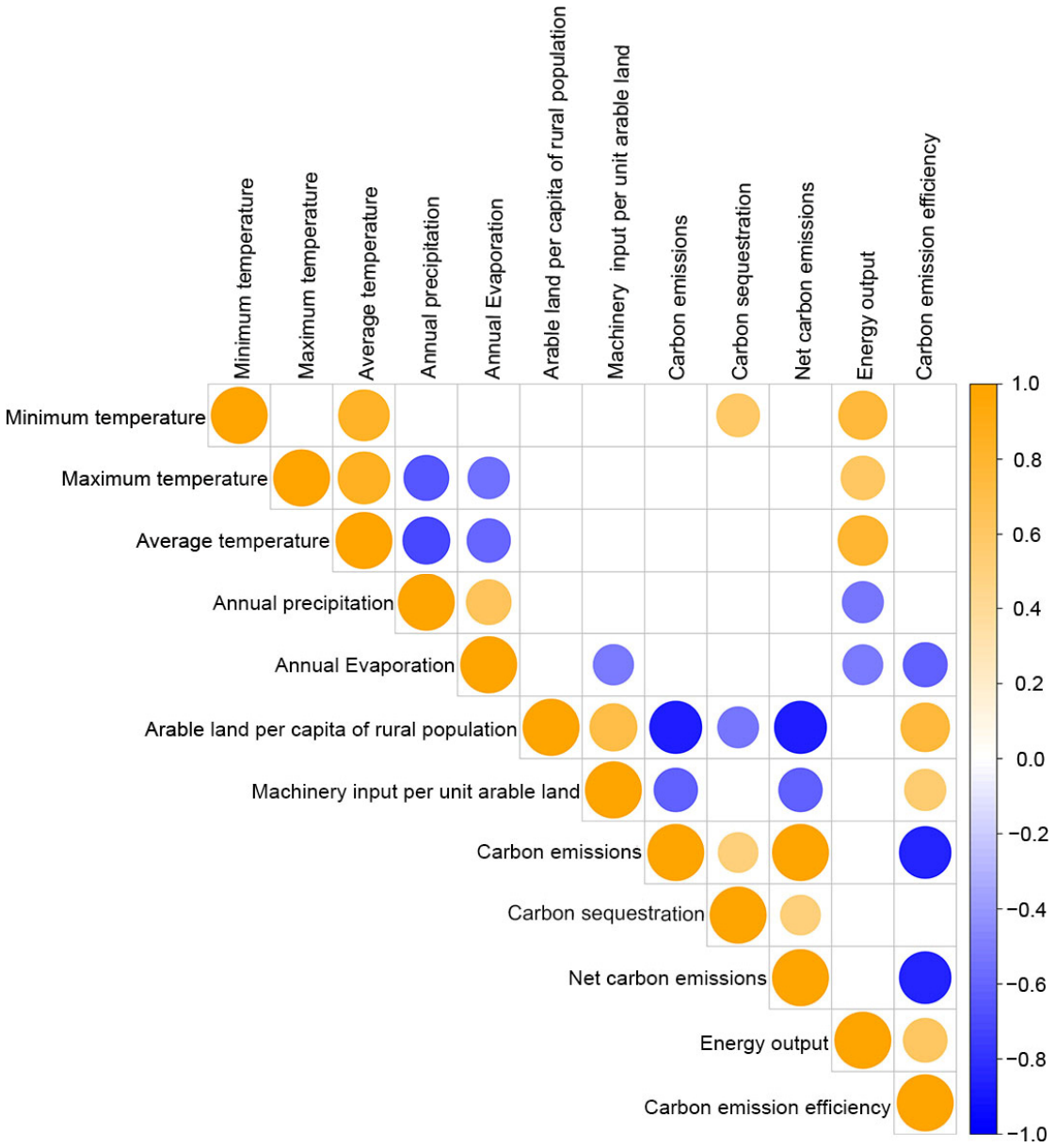


Figure 5. Carbon emission indices (carbon emission, carbon sequestration, energy output, net carbon emissions, carbon emission efficiency), cropland management scale (arable land per capita of rural population), agricultural mechanization (machinery input per unit arable land), and climate factors (minimum temperature, maximum temperature, average temperature, annual precipitation, and annual evaporation) are all represented graphically in a correlation matrix using the Spearman correlation coefficient. Positive correlations are shown by orange, whereas negative correlations are shown by blue. The size of the circles and the color intensity show how strongly the relationships exist. Non-significant correlations ($p > 0.05$) are indicated by empty cells.

The correlations between carbon emission indices and climate change, cropland management scale, and agricultural machination were also analyzed. Concerning climate change, the minimum temperature was strongly and positively correlated with carbon sequestration (r = 0.59), indicating the increase in minimum temperature may cause a growth of carbon sequestration; the minimum temperature (r = 0.74), maximum temperature (r = 0.61), and average temperature (r = 0.78) were strongly and positively correlated with energy output, while annual precipitation (r = −0.54) and annual evaporation (r = −0.51) were strongly and negatively correlated with energy output, indicating pos-

itive factors of temperature and negative factors of precipitation and evaporation; the annual evaporation was strongly and negatively correlated with carbon emission efficiency ($r = -0.62$), suggesting that the carbon emissions efficiency decreases with increasing annual evaporation. Concerning the cropland management scale, arable land per capita of rural population was strongly and negatively correlated with carbon emissions ($r = -0.86$), carbon sequestration ($r = -0.53$), and net carbon emissions ($r = -0.86$), indicating the bigger the cropland management scale, the lower carbon emissions, carbon sequestration, and net carbon emissions. Meanwhile, arable land per capita of rural population was strongly and positively correlated with carbon emission efficiency ($r = 0.75$), showing the bigger the cropland management scale, the higher the carbon emission efficiency. Concerning agricultural machination, machinery input per unit of arable land was strongly and negatively correlated with carbon emissions ($r = -0.60$) and net carbon emissions ($r = -0.60$), while it was strongly and positively correlated with carbon emission efficiency ($r = 0.54$), showing that the higher the agricultural machination, the lower the carbon emissions but the higher the carbon emission efficiency.

In addition, the average temperature was strongly and positively correlated with minimum temperature ($r = 0.82$) and maximum temperature ($r = 0.85$). The annual precipitation was strongly and positively correlated with annual evaporation ($r = 0.64$). However, maximum temperature and average temperature were strongly and negatively correlated with annual precipitation and annual evaporation, showing that the higher the temperature, the lower the annual precipitation and evaporation.

4. Discussion

4.1. The Carbon Emissions of the Whole Study Area

Over the entire study period from 2001 to 2020, the trend in energy output was not significant; however, net carbon emissions exhibited a notable downward trend, consistent with the findings of Zhang et al. [20], which showed a decrease in carbon emissions from cropland between 2000 and 2019. This decline in emissions led to a substantial improvement in carbon emission efficiency for the region. Figure 3a and Table 2 show that the carbon emission decreased mainly because of the decrease in chemical fertilizer input and straw burning. This is related to a series of measures introduced by the Ministry of Agriculture and Rural Affairs of the People's Republic of China, such as the "Zero Growth Action Plan of Fertilizer Use by 2020" issued in 2015 and the "Action Plan for Fertilizer Reduction by 2025" issued in 2022 [30,31]. Also, burning straw was prevented with the Law of the People's Republic of China on the Prevention and Control of Atmospheric Pollution published and enforced in 2016, and returning straw has been advocated [32]. Despite the downward trend in agricultural inputs to the coastal saline cropland ecosystem in the recent 20 years, the primary contributors to GHG were still electricity, chemical N fertilizer, nitrogen input, and returning straw. Similar to cropland ecosystems at the national level, these emission sources made for 65.06% of the total emissions [9]. The Yellow River Delta is a typical irrigation area, requiring more electricity for crop irrigation and leaching soil salt. Facing the nutrient deficiency problem in the saline cropland ecosystem [33], the farmers usually input a large amount of chemical N fertilizer to obtain a higher crop yield [29].

Concerning the net carbon emissions of the whole study area, the average value was 10.25 ton CO_2-eq ha^{-1}, which is higher than the main grains (rice: 8.60 ton CO_2-eq ha^{-1}; wheat: 3.70 ton CO_2-eq ha^{-1}; maize: 3.30 ton CO_2-eq ha^{-1}) at the national level of China [34]. In addition, the grain yield of the Yellow River Delta was 5318 kg ha^{-1} in 2020 [22], which was lower than the average grain yield of the whole Shandong province, i.e., 6577 kg ha^{-1} [35]. Therefore, the carbon emission efficiency in the coastal saline cropland ecosystem was lower than that of the average level in the grain-producing area.

4.2. The Carbon Emissions in Different Regions with Different Soil Salinization

The carbon emissions pattern was related to the level of soil salinization. The average values of carbon emissions, carbon sequestration, net carbon emissions, energy output,

and carbon emission efficiency all increased with the increase in soil salinization (Table 2). The low-salinization regions were characterized by high emissions, high sequestration, high productivity, and high carbon emission efficiency. The high-salinization regions were characterized by low emissions, low sequestration, and low productivity, and low carbon emission efficiency. Although carbon emission efficiency exhibited significant increasing trends across high-, moderate-, and low-salinization regions from 2001 to 2020, there remains considerable potential for further improvement in cropland ecosystems in all soil salinization regions through the adoption of region-specific strategies. Concerning *regions with high salinization*, energy outputs were 4.91 $\times$ 10^7 kJ ha^{-1}, significantly lower than those in low-salinization regions (16.65 $\times$ 10^7 kJ ha^{-1}), where higher carbon emission efficiency was observed (Table 2). Therefore, enhancing land productivity should be the primary goal for these regions. Moreover, carbon sequestration in regions with high salinization showed a significant upward trend, and its values remained substantially lower than in low-salinization regions. To address this, soil improvement technologies [17,18] and the cultivation of salt-tolerant crop varieties [19] could be employed to boost crop biomass and soil carbon sequestration. Concerning *regions with low salinization*, both carbon emissions and net carbon emissions have shown significant declining trends, but they remain considerably higher than in high-salinization regions. This indicates that these areas have significant potential for further emissions reduction. Strategies such as improving nitrogen and water use efficiency could be particularly effective in these regions.

4.3. The Driving Factors of Carbon Emissions

Given the whole agricultural production pattern, the Yellow River Delta region obtains high output through high input and high emissions [29]. Our results showed a synergic relationship between carbon emissions, carbon sequestration, and net carbon emission, which is consistent with the agricultural production pattern in the Yellow River Delta region. However, soil salinization leads to low use efficiency of fertilizer, and high underground water levels result in serious nitrate leaching, contaminating the groundwater in the Yellow River Delta region [29]. Therefore, lowering nitrate leaching and increasing nitrogen use efficiency are crucial steps to lower carbon emissions and boost carbon sequestration in the Yellow River Delta.

The local climate has a major role in determining agricultural productivity because crop growth area is controlled by meteorological conditions [36]. Crop yield is affected by climate change differently in different places; in some, it will increase, while in others, it will decrease [37]. Our results showed a positive correlation between temperature indices and energy output, indicating temperature increase caused a growth of productivity in the coastal saline cropland ecosystem. Indeed, an increase in temperature could extend the potential growing season by altering expected frost dates, thereby leading to increased crop yields [38]. Additionally, elevated CO_2 levels can have a compensatory effect on the yields of C3 crops, such as wheat and rice [38]. However, increased precipitation and high evaporation rates can lower energy output and reduce carbon emission efficiency. In coastal saline cropland ecosystems, saltwater intrusion and intensified human activities contribute to poor soil permeability. Consequently, heavy precipitation can lead to waterlogging, which in turn reduces crop yields [39] and further decreases carbon emission efficiency. Additionally, high evaporation rates, particularly in regions with limited water resources, can deplete soil moisture, further stressing crops and leading to a decline in overall productivity [40].

Moreover, the cropland management scale is an important factor to carbon emissions and carbon emission efficiency in the coastal saline cropland ecosystems. In our study, a negative correlation was found between arable land per capita of rural population and carbon emissions and net carbon emissions in the Yellow River Delta region, indicating that the larger the cropland management scale, the lower the carbon emissions. While there is a positive relationship between carbon emission efficiency and arable land per capita of rural population, indicating that the greater the cropland management scale, the greater

the carbon emission efficiency. These findings aligned with those of Zhu et al. [14], and large-scale cropland management can increase the carbon emission efficiency.

Moreover, agricultural mechanization is also a factor in carbon efficiency. In our study, a negative correlation between machinery input per unit arable land and carbon emissions, while a positive correlation between machinery input per unit arable land and carbon emission efficiency, was identified in the Yellow River Delta regions, showing the higher the degree of agricultural mechanization, the lower the carbon emissions and the higher the carbon emission efficiency. Machinery input is one of the carbon emission sources; however, it can also increase the crop yield. According to Peng et al. [41], the yield of grain crops increases by 1.59% for every 1.00% increase in the level of agricultural mechanization. Currently, for the whole of the Yellow River delta region, increasing agricultural mechanization will be beneficial to the carbon emission efficiency of the coastal saline cropland ecosystem.

4.4. Limitations and Perspectives of the Study

This study uses the Yellow River Delta as a case study to analyze the temporal and spatial trends, as well as the driving factors, of the carbon footprint in coastal saline cropland ecosystems. However, there are several limitations and perspectives to consider. Firstly, although we calculated GHG emissions from agricultural inputs using the latest emission factors based on similar studies in comparable areas, there are differences in emission factors across various agricultural input types. For example, the emission factors for electricity vary depending on the source of power generation, such as thermal, hydro, or wind energy. These emission factors could be further refined through targeted surveys. Secondly, our study focuses on the region as a whole and estimates GHG emissions across different regional types, but it does not account for the impact of farmer behavior on GHG emissions. A household survey on the use of fertilizers, pesticides, and machinery could provide deeper insights into the emission mechanisms.

5. Conclusions

This study examined the CF's driving factors and temporal and spatial trends in the Yellow River Delta. Concerning the whole study area, the energy output was almost unchanged during 2001–2020, while the net carbon emissions showed a significant downward trend, causing a significant increase in the carbon emission efficiency. The agricultural production pattern was characterized by high input, high emissions, and high output in the Yellow River Delta region. Electricity, chemical N fertilizer, nitrogen input, and returning straw were the main sources of carbon emissions, which accounted for 65.06% of the total emissions. Carbon emission indices showed differences in different soil salinization regions. The high-salinization regions were characterized by low emissions, low sequestration, low productivity, and low carbon emission efficiency, while the low-salinization regions were characterized by high emissions, high sequestration, high productivity, and high carbon emission efficiency. A synergic relationship between carbon emissions, carbon sequestration, and net carbon emission was found in the Yellow River Delta region. The temperature indices were the positive factors in energy output, while annual precipitation and evaporation were the negative factors in energy output. The cropland management scale and agricultural mechanization were the negative factors in carbon emissions and net carbon emissions but were the positive factors in carbon emission efficiency.

Based on our findings, three key principles have been proposed for policy recommendations to enhance carbon emission efficiency. First, tailored strategies for different salinization levels. Regions with varying degrees of salinization should implement targeted strategies. In high-salinization areas, the focus should be on boosting land productivity and enhancing soil carbon sequestration. In contrast, low-salinization regions should prioritize efforts to reduce carbon emissions. Second, strengthening cropland drainage infrastructure is essential to mitigate the adverse effects of heavy rainfall, ensuring more stable and productive agricultural systems. Third, expanding the scale of cropland management through

land transfers and promoting agricultural mechanization can substantially improve production efficiency, thereby enhancing carbon emission efficiency. These recommendations could provide valuable insights for policymakers and agricultural professionals aiming to achieve carbon peak and carbon neutrality in saline cropland ecosystems.

Supplementary Materials: The following supporting information can be downloaded at: https://www.mdpi.com/article/10.3390/land13122145/s1, Table S1: The N_2O emissions by soil respiration without fertilization in different crops land; Table S2: Harvest index, ratio of underground biomass to aboveground biomass, nitrogen content of straw and root, the proportion of straw burned to the total straw biomass, and the proportion of straw return to the total straw biomass; Table S3: Greenhouse gases emissions from straw burning by crops per unit weight; Table S4: Energy conversion coefficient of crops. Refs. [9,27,42–49] are cited in Supplementary Materials document.

Author Contributions: Conceptualization, Y.L. and G.W.; methodology, Y.L.; software, Y.L.; validation, D.Z., Y.W., X.L., Y.Z. and G.W.; formal analysis, Y.L.; investigation, D.Z. and Y.W.; data curation, Y.L.; writing—original draft preparation, Y.L.; writing—review and editing, D.Z., Y.W., X.L., Y.Z. and G.W.; visualization, Y.L. and G.W.; supervision, G.W.; project administration, Y.L.; funding acquisition, Y.L. All authors have read and agreed to the published version of the manuscript.

Funding: This research was funded by the Natural Science Foundation of Shandong Province (grant number: ZR2022QC148) and the National Natural Science Foundation of China (grant number: 42407607).

Data Availability Statement: Data will be made available upon reasonable request.

Conflicts of Interest: The authors declare no conflicts of interest.

References

1. Cui, Q.; Xia, J.; Yang, H.; Liu, J.; Shao, P. Biochar and effective microorganisms promote Sesbania cannabina growth and soil quality in the coastal saline-alkali soil of the Yellow River Delta, China. *Sci. Total Environ.* **2021**, *756*, 143801. [CrossRef] [PubMed]
2. Daliakopoulos, I.; Tsanis, I.; Koutroulis, A.; Kourgialas, N.; Varouchakis, A.; Karatzas, G.; Ritsema, C. The threat of soil salinity: A European scale review. *Sci. Total Environ.* **2016**, *573*, 727–739. [CrossRef] [PubMed]
3. Yuneng, D.; Youliang, X.; Leiyong, Z.; Shufang, S. Can China's food production capability meet her peak food demand in the future? Based on food demand and production capability prediction till the year 2050. *Int. Food Agribus. Manag. Rev.* **2020**, *23*, 1–17. [CrossRef]
4. Li, Y.; Sun, Z.; Accatino, F. Spatial distribution and driving factors determining local food and feed self-sufficiency in the eastern regions of China. *Food Energy Secur.* **2021**, *10*, e296. [CrossRef]
5. Yang, W.; Yang, M.; Wen, H.; Jiao, Y. Global Warming Potential of CH_4 uptake and N_2O emissions in saline–alkaline soils. *Atmos. Environ.* **2018**, *191*, 172–180. [CrossRef]
6. Yan, M.; Cheng, K.; Luo, T.; Yan, Y.; Pan, G.; Rees, R.M. Carbon footprint of grain crop production in China–based on farm survey data. *J. Clean. Prod.* **2015**, *104*, 130–138. [CrossRef]
7. Yang, X.; Gao, W.; Zhang, M.; Chen, Y.; Sui, P. Reducing agricultural carbon footprint through diversified crop rotation systems in the North China Plain. *J. Clean. Prod.* **2014**, *76*, 131–139. [CrossRef]
8. Xu, X.; Lan, Y. A comparative study on carbon footprints between plant-and animal-based foods in China. *J. Clean. Prod.* **2016**, *112*, 2581–2592. [CrossRef]
9. Chen, X.; Ma, C.; Zhou, H.; Liu, Y.; Huang, X.; Wang, M.; Cai, Y.; Su, D.; Muneer, M.A.; Guo, M. Identifying the main crops and key factors determining the carbon footprint of crop production in China, 2001–2018. *Resour. Conserv. Recycl.* **2021**, *172*, 105661. [CrossRef]
10. Liu, W.; Zhang, G.; Wang, X.; Lu, F.; Ouyang, Z. Carbon footprint of main crop production in China: Magnitude, spatial-temporal pattern and attribution. *Sci. Total Environ.* **2018**, *645*, 1296–1308. [CrossRef]
11. Xu, X.; Lan, Y. Spatial and temporal patterns of carbon footprints of grain crops in China. *J. Clean. Prod.* **2017**, *146*, 218–227. [CrossRef]
12. Lesk, C.; Rowhani, P.; Ramankutty, N. Influence of extreme weather disasters on global crop production. *Nature* **2016**, *529*, 84–87. [CrossRef]
13. Ren, C.; Liu, S.; Van Grinsven, H.; Reis, S.; Jin, S.; Liu, H.; Gu, B. The impact of farm size on agricultural sustainability. *J. Clean. Prod.* **2019**, *220*, 357–367. [CrossRef]
14. Zhu, Y.; Waqas, M.A.; Zou, X.; Jiang, D.; Wilkes, A.; Qin, X.; Gao, Q.; Wan, Y.; Hasbagan, G. Large-scale farming operations are win-win for grain production, soil carbon storage and mitigation of greenhouse gases. *J. Clean. Prod.* **2018**, *172*, 2143–2152. [CrossRef]
15. Yang, T.; Huang, X.; Wang, Y.; Li, H.; Guo, L. Dynamic linkages among climate change, mechanization and agricultural carbon emissions in rural China. *Int. J. Environ. Res. Public Health* **2022**, *19*, 14508. [CrossRef]

16. Li, Y.; Xu, L.; Qi, F.; Gao, H.; Yu, S.; Fu, T.; Liu, J. Seepage field simulation of subsurface pipe salt drainage processes in coastal saline-alkali farmland. *Chin. J. Eco-Agric.* **2023**, *31*, 1110–1120.
17. Liu, X.; Yang, J.; Tao, J.; Yao, R.; Li, W.; Xie, W.; Wang, X. Effects of the combined application of biochar and humic substances on the improvement of saline cropland in the Yellow River Delta of China. *Land Degrad. Dev.* **2023**, *34*, 4793–4809. [CrossRef]
18. Sun, Y.; Chen, X.; Yang, J.; Luo, Y.; Yao, R.; Wang, X.; Xie, W.; Zhang, X. Coastal Soil Salinity Amelioration and Crop Yield Improvement by Biomaterial Addition in East China. *Water* **2022**, *14*, 3266. [CrossRef]
19. Tao, R.; Ding, J.; Li, C.; Zhu, X.; Guo, W.; Zhu, M. Evaluating and screening of agro-physiological indices for salinity stress tolerance in wheat at the seedling stage. *Front. Plant Sci.* **2021**, *12*, 646175. [CrossRef]
20. Zhang, C.-y.; Zhao, L.; Zhang, H.; Chen, M.-n.; Fang, R.-y.; Yao, Y.; Zhang, Q.-p.; Wang, Q. Spatial-temporal characteristics of carbon emissions from land use change in Yellow River Delta region, China. *Ecol. Indic.* **2022**, *136*, 108623. [CrossRef]
21. Li, Q.; Chen, Q.; Lv, R.; Liu, W.; Zhao, L.; Zhang, J.; Guo, Q.; Qiu, X.; You, H. Spring soil CO_2 and CH_4 emissions in the Yellow River Delta wetland, China. *J. Sea Res.* **2022**, *190*, 102280. [CrossRef]
22. DYSY. *Dongying Statistical Yearbook*; Dongying Statistics Bureau: Dongying, China, 2021.
23. Chen, S.; Lu, F.; Wang, X. Estimation of greenhouse gases emission factors for China's nitrogen, phosphate, and potash fertilizers. *Acta Ecol. Sin.* **2015**, *35*, 6371–6383.
24. Chen, X.; Cui, Z.; Fan, M.; Vitousek, P.; Zhao, M.; Ma, W.; Wang, Z.; Zhang, W.; Yan, X.; Yang, J. Producing more grain with lower environmental costs. *Nature* **2014**, *514*, 486–489. [CrossRef]
25. Yang, S.; Wang, C.; Huo, L.; Jiang, W.; Wen, M. Effects of different tillage practices on soil organic carbon of cultivated land in Gansu Yellow River irrigation district. *Trans. Chin. Soc. Agric. Eng.* **2019**, *35*, 114–121.
26. IPCC. *Climate Change 2021: The Physical Science Basis: Working Group I Contribution to the Fifth Assessment Report of the Intergovernmental Panel on Climate Change*; Cambridge University Press: Cambridge, UK, 2021.
27. CNDRC. *China National Development and Reform Commission. Guidelines for the Preparation of Provincial GHG Inventories (Trial)*; China National Development and Reform Commission: Beijing, China, 2011.
28. Muñoz Sabater, J. ERA5-Land Monthly Averaged Data from 1950 to Present [Internet]. Copernicus Climate Change Service (C3S) Climate Data Store (CDS). 2019. Available online: https://cds.climate.copernicus.eu/datasets/reanalysis-era5-land-monthly-means?tab=overview (accessed on 17 November 2023).
29. Ouyang, Z.; Wang, H.; Lai, J.; Wang, C.; Liu, Z.; Sun, Z.; Hou, R. New Approach of High-quality Agricultural Development in the Yellow River Delta. *Bull. Chin. Acad. Sci.* **2020**, *35*, 145–153.
30. Van Wesenbeeck, C.; Keyzer, M.; Van Veen, W.; Qiu, H. Can China's overuse of fertilizer be reduced without threatening food security and farm incomes? *Agric. Syst.* **2021**, *190*, 103093. [CrossRef]
31. MARAPRC. Ministry of Agriculture and Rural Affairs of the People's Republic of China. *Notice of the Issuance of the Action Plan for the Reduction of Chemical Fertilizers by 2025 and the Action Plan for the Reduction of Chemical Pesticides by 2025*; MARAPRC: Beijing, China, 2022. Available online: http://www.moa.gov.cn/nybgb/2022/202212/202301/t20230104_6418252.htm (accessed on 4 January 2023).
32. Wang, Y.-J.; Wang, N.; Huang, G.Q. How do rural households accept straw returning in Northeast China? *Resour. Conserv. Recycl.* **2022**, *182*, 106287. [CrossRef]
33. He, K.; He, G.; Wang, C.; Zhang, H.; Xu, Y.; Wang, S.; Kong, Y.; Zhou, G.; Hu, R. Biochar amendment ameliorates soil properties and promotes Miscanthus growth in a coastal saline-alkali soil. *Appl. Soil Ecol.* **2020**, *155*, 103674. [CrossRef]
34. Tian, P.; Lu, H.; Heijungs, R.; Li, D.; Xue, Y.; Yang, Y. Patterns of carbon footprints of main grains production in China: A comparison between main and non-main producing areas. *Environ. Sci. Pollut. Res.* **2022**, *29*, 23595–23606. [CrossRef]
35. SDSY. *Shandong Statistical Yearbook*; Shandong Statistics Bureau: Jinan, China, 2021.
36. Fatima, Z.; Naz, S.; Iqbal, P.; Khan, A.; Ullah, H.; Abbas, G.; Ahmed, M.; Mubeen, M.; Ahmad, S. Field crops and climate change. In *Building Climate Resilience in Agriculture: Theory, Practice and Future Perspective*; Springer: Cham, Switzerkand, 2022; pp. 83–94.
37. Kang, Y.; Khan, S.; Ma, X. Climate change impacts on crop yield, crop water productivity and food security—A review. *Prog. Nat. Sci.* **2009**, *19*, 1665–1674. [CrossRef]
38. Rezaei, E.E.; Webber, H.; Asseng, S.; Boote, K.; Durand, J.L.; Ewert, F.; Martre, P.; MacCarthy, D.S. Climate change impacts on crop yields. *Nat. Rev. Earth Environ.* **2023**, *4*, 831–846. [CrossRef]
39. Tian, L.-X.; Zhang, Y.-C.; Chen, P.-L.; Zhang, F.-F.; Li, J.; Yan, F.; Dong, Y.; Feng, B.-L. How does the waterlogging regime affect crop yield? A global meta-analysis. *Front. Plant Sci.* **2021**, *12*, 634898. [CrossRef] [PubMed]
40. Bodner, G.; Nakhforoosh, A.; Kaul, H.P. Management of crop water under drought: A review. *Agron. Sustain. Dev.* **2015**, *35*, 401–442. [CrossRef]
41. Peng, J.; Zhao, Z.; Liu, D. Impact of agricultural mechanization on agricultural production, income, and mechanism: Evidence from Hubei province, China. *Front. Environ. Sci.* **2022**, *10*, 838686. [CrossRef]
42. Chen, L.; Xue, L.; Xue, Y. Spatial agglomeration and variation of China's agricultural net carbon sink. *Ecol. Environ. Sci.* **2015**, *24*, 1777–1784.
43. IPCC. N_2O emissions from managed soils, and CO_2 emssions from lime and urea application. In *2019 Refinement to the 2006 IPCC Guidelines for National Greenhouse Gas Inventories*; Cambridge University Press: Cambridge, UK; New York, NY, USA, 2019; Chapter 11.
44. Li, Y.; Sun, Z.; Zhang, X.; Yang, J.; Hang, S.; Li, S.; Zhu, W.; Lyu, Y.; Ouyang, Z. Spatial pattern and evolutionary trend of sustainable development index of crop-livestock system: A case study in Shandong Province, China. *Chin. J. Appl. Ecol.* **2019**, *30*, 2371.

45. Min, J.; Hu, H. Calculation of Greenhouse Gases Emission from Agricultural Production in China. *China Popul. Ressour. Environ.* **2012**, *22*, 21–27.
46. Wei, L.; Wang, Z.; Li, L.; Hou, H.; Lou, J. Comparative test of different rice varieties in the Yellow River Delta. *North Rice* **2017**, *47*, 11–14.
47. Xie, G.; Han, D.; Wang, X.; Lv, R. Harvest index and residue factor of cereal crops in China. *J. China Agric. Univ.* **2011**, *16*, 9–17.
48. Xie, G.; Wang, X.; Han, D.; Xue, S. Harvest index and residue factor of non-cereal crops in China. *J. China Agric. Univ.* **2011**, *16*, 9–17.
49. Zhang, Q.; Ju, X.; Zhang, F. Re-estimation of direct nitrous oxide emission from agricultural soils of China via revised IPCC2006 guideline method. *Chin. J. Eco-Agric.* **2010**, *18*, 7–13. [CrossRef]

Disclaimer/Publisher's Note: The statements, opinions and data contained in all publications are solely those of the individual author(s) and contributor(s) and not of MDPI and/or the editor(s). MDPI and/or the editor(s) disclaim responsibility for any injury to people or property resulting from any ideas, methods, instructions or products referred to in the content.